Theor Appl Climatol (2016) 125:131–147
DOI 10.1007/s00704-015-1493-z

ORIGINAL PAPER

Long-term trends in daily precipitation over the Yangtze River Delta region during 1960–2012, Eastern China

Chunsheng Hu[1] · **Youpeng Xu**[1] · **Longfei Han**[1] · **Liu Yang**[1] · **Guanglai Xu**[1]

Received: 30 December 2014 / Accepted: 24 April 2015 / Published online: 12 May 2015

Abstract Based on daily precipitation data from 24 stations over the Yangtze River Delta (YRD) region, the long-term trends of daily precipitation are analyzed during the period 1960–2012 using 12 precipitation indices. The results indicate that the following. (1) For the regional average trends of precipitation, nine indices [i.e., RR, SDII, PCI(day), R25mm, R50mm, R25mmT, R50mmT, R25mmTOT, and R50mmTOT] show the increasing trends, while three indices [i.e., RX1day, RR1 and PCI(month)] display the decreasing trends. Furthermore, the annual total precipitation (RR) is correlated strongly with most of the other precipitation indices, especially indices represent the heavy precipitation which is responsible for more than 90 % of the total increase of precipitation. (2) The central and southern parts of the study area become more humid than the northern parts, although the daily precipitation undergo a consistent concentrated trend over almost all of the study area. Moreover, the frequency and contribution of the heavy precipitation also arise dramatically in almost the entire study area, and the precipitation events show the significant trend of extremeness. (3) The abrupt changes for RR, RX1day, SDII, R50mm, R50mmT, and R50mmTOT are detected in 1984, 1988, 1987, 1984, 1988, and 1988, respectively, which indicate the abrupt change of precipitation occurred consistently in the mid-1980s. Three major cycles of precipitation detected are 5–6-year cycle, 13-year cycle, and 20-year cycle, with a nonsignificant 2-year cycle coexisted. In addition, a significant change of cycles occurred in the 1980s, when the short cycle was set to overtake the long cycle, resulting in high-frequency and instability of precipitation changes over the YRD region in recent decades. (4) There are three factors (the global warming, the East Asian summer monsoon change, and the urbanization development) might potentially impact on the frequency and volume of precipitation. The variation of East Asian summer monsoon is the key factor that influences the increase of precipitation, while the global warming and the urbanization development perform the background factor and the local factor, respectively.

1 Introduction

Climate change has been the topic of many research studies over the world during the twentieth century (Alexander et al. 2006; IPCC 2007). For the environmental and economic conditions, the precipitation is an important driver of the dynamics of climate and the biosphere, and is of great practical importance to society, with multiple impacts on the environment and human life (Mishra and Singh 2010). However, changes in precipitation parameters are not well understood presently because it is commonly accepted that the factors influencing precipitation are complex and vary regionally (López-Moreno et al. 2010). Therefore, changes in precipitation have attracted many attentions of the researchers in different regions over the world, and most studies have addressed the changes in precipitation across different regions and timescales, i.e., Europe (Zolina et al. 2010; Altava-Ortiz et al. 2011; de Lima et al. 2013; Altin and Barak 2014), America (Shepherd 2006; Carrera-Hernández and Gaskin 2007; Martinez et al. 2012; Petrie et al. 2014), Asia (Zhang et al. 2009; Xu et al. 2010; Wang 2012; Pathirana et al. 2014), and Africa (Gaughan and Waylen 2012; Roy and Rouault 2013; Sarr et al. 2013;

✉ Youpeng Xu
xuyp305@163.com

[1] School of Geographic and Oceanographic Sciences, Nanjing University, Nanjing 210023, China

Weldeab et al. 2014). The previous studies showed that the anthropic activities are one of the important factors promoting the complexity of changes in precipitation with exception of natural factors, especially in the area of rapid urbanization.

The Yangtze River Delta (YRD) region is one of the most economically developed regions in China, and still maintains a rapid growth momentum presently. The importance of selecting the YRD region as the study area is due to the dramatic economic growth, high-density population, rapid urbanization, and the increasing flood disasters in this region (Xu et al. 2010). Many studies have been conducted in or near the YRD region on the changes of precipitation. For instance, Zhai et al. (2005) pointed out that significant increases in extreme precipitation and annual total precipitation had been found in the mid-lower reaches of Yangtze River for the period 1951–2000. Mei and Yang (2005) revealed that the trend for precipitation amount in spring and summer was significantly negative and positive, respectively, while the obvious trend for annual precipitation amount was not found. Lv et al. (2009) indicated that the precipitation over the middle-lower reaches of Yangtze River had experienced five interdecadal regime shifts during 1900–2006, and the precipitation underwent an interdecadal increase in the early 1980s. Zhang et al. (2009) suggested that the middle and the lower sections of Yangtze River were dominated by increasing annual, summer, and winter precipitation in generally. Xu et al. (2010) investigated the impacts of urbanization on precipitation, hydrological process, and water environment in some typical cities. The results showed that the annual precipitation and the flood season precipitation in the urban areas exhibited a striking increase, with the rapid development of urbanization. Zhao et al. (2011) also analyzed the urbanization effects on precipitation in the YRD region using the satellite data and explored that the urbanization might be a critical impact factor of increasing precipitation. Pan et al. (2011) examined the trend of precipitation variation in the YRD region from 1961 to 2006 with the help of the meteorological data of 84 stations and found that the annual precipitation did not show any significant trend, while the seasonal distribution of the precipitation exhibited significant changes. Jiang et al. (2012) discussed climate changes and possible reasons in the YRD region from 1960 to 2010 and suggested that the climate changes in the YRD region significantly related to urbanization, air–sea interaction, and the main synoptic system. Sang et al. (2013) investigated into the daily precipitation variability in the YRD region, based on 58 stations from 1958 to 2007, and also discussed the effects of urbanization on precipitation. He et al. (2013) found that all of precipitation indices presented increasing tendency except the precipitation intensity in past 50 years, and both of the number of heavy precipitation days and maximum 1-day precipitation increased obviously over the middle and lower reaches of Yangtze River. Zhang et al. (2013) found that distinct decreases in rainfall days were observed over most parts of the Yangtze River Basin, but precipitation intensity increased over most parts of the Yangtze River Basin, particularly in the Lower Yangtze River Basin. Wang et al. (2013) analyzed the spatial and temporal patterns of the precipitation concentration in the Yangtze River Basin for the period 1960–2008 and revealed that the lower value of precipitation concentration index was located in the lower region of the Yangtze River Basin.

As mentioned above, the previous studies in the YRD region mainly focus on the variability of monthly, seasonal, and annual precipitation, while there is a lack of study on the variability of daily precipitation, which is very important for studying precipitation regime and heavy precipitation. Moreover, the previous studies are less involved in researches on the abrupt changes and periodicity features of precipitation, which are very helpful to interpret the shift of precipitation patterns and predict the future states of precipitation. Therefore, based on 12 precipitation indices, this study uses the daily precipitation data as of 2012 and measured from 24 meteorological stations, mainly to investigate long-term trends of daily precipitation in detail over the YRD region during 1960–2012. The purposes of this study are (1) to investigate the variability of daily precipitation, (2) to explore the abrupt changes and periodicity features of the precipitation, and (3) to discuss the causes of the precipitation changes.

2 Study area and data

2.1 Study area

The YRD region, which is one of the most development regions in China with a population of about 156 million, locates between 27.16–35.13° N latitude and 116.36–122.13° E longitude and covers an area of about 207,300 km^2. The study area consists of Shanghai, Jiangsu, and Zhejiang provinces (Fig. 1), known as the economy Yangtze River Delta. The YRD region is a delta with typical plain river network in China, which dotted crisscrossed rivers and dense water system (Xu et al. 2010). The low and flat terrain of the YRD region has an average elevation of <10 m, with some mountains in the south. The study area is a typical monsoonal climate region controlled by the East Asian monsoon, and the southern YRD region is warmer and wetter than the north (Svensson 1999). However, with the dramatic economic growth, densest population, and rapid urbanization in recent decades, the YRD region is facing serious problems of heavy precipitation, flood risk, water quality deterioration, water shortage, etc., which seriously threaten the living environment of the area.

2.2 Data

Daily precipitation data are collected from 24 national standard meteorological stations (Fig. 1). The data of daily precipitation

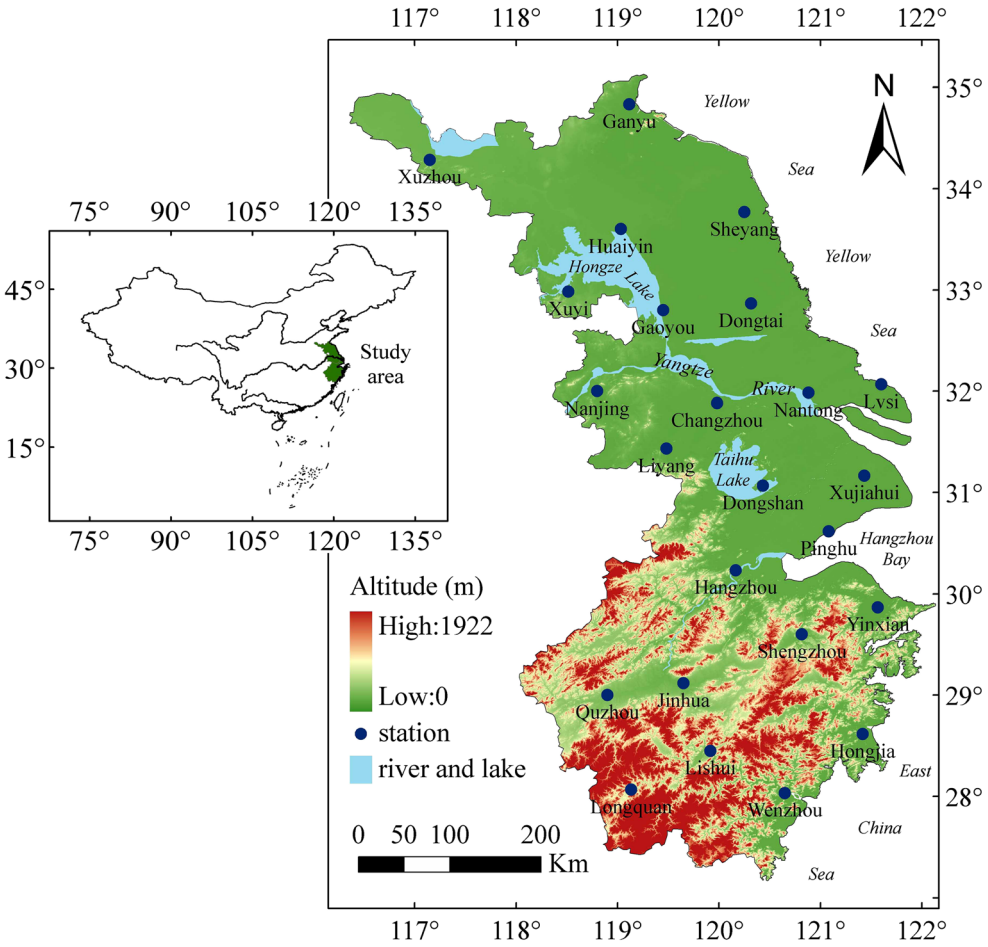

Fig. 1 Locations of the Yangtze River Delta region and meteorological stations

are provided by the National Climate Center of China Meteorological Administration (CMA). The meteorological stations are identified according to their world Meteorological Organization numbers, names, latitudes, longitudes, and altitudes (Table 1). The data quality is strictly controlled before its release. The period of records of most stations used in this study is 1960–2012, except the Huaiyin, Xujiahui, Wenzhou, and Longquan station, which is available in 1960–2008. Therefore, the missing values of these four stations are further interpolated using the nearest stations (i.e., Huaian, Baoshan, Ruian, and Yunhe) for the period 2009–2012.

3 Methodology

3.1 Precipitation indices

The study of precipitation trends is done by analyzing the time series of precipitation indices. The precipitation indices selected for the study are described in Table 2. Those selected indices were widely employed to estimate the changes in daily precipitation in different areas during the past decade (Alexander et al. 2006; Fatichi and Caporali 2009; Cao and Pan 2014). The indices are calculated for the precipitation of each individual station and also for the areal mean precipitation in the study area (i.e., the YRD region). The selected indices are classified into two categories in this study. The first category is indices of the general precipitation (i.e., RR, RX1d, RR1, SDII, and PCI). The other category is indices of the heavy precipitation (i.e., R25mm, R50mm, R25mmT, R50mmT, R25mmTOT, and R50mmTOT). In this study, the heavy precipitation, which is defined as the precipitation events with precipitation amount ≥25 mm/day, is divided into two types, the heavy rain (50 mm/day>preicipitation≥25 mm/day) and the torrential rain (or storm) (precipitation≥50 mm/day), respectively (Domrös and Peng 1988; Wu et al. 2008).

3.2 Mann–Kendall test

3.2.1 Mann–Kendall test of trends

The Mann–Kendall trend test is based on the correlation between the ranks of a time series (i.e., $X=\{x_1, x_2, \ldots, x_n\}$) and their order (Mann 1945; Kendall 1975). The Mann–Kendall test statistic is given as:

Table 1 Information on the meteorological stations analyzed in this study

No. of station	Name	Latitude (°N)	Longitude (°E)	Altitude (m)
58027	Xuzhou	34.28	117.15	41.2
58040	Ganyu	34.83	119.12	3.3
58138	Xuyi	32.98	118.52	40.8
58144	Huaiyin	33.60	119.03	17.5
58150	Sheyang	33.77	120.25	2.0
58238	Nanjing	32.00	118.80	7.1
58241	Gaoyou	32.80	119.45	5.4
58251	Dongtai	32.87	120.32	4.3
58259	Nantong	31.98	120.88	6.1
58265	Lvsi	32.07	121.60	5.5
58343	Changzhou	31.88	119.98	4.4
58345	Liyang	31.43	119.48	7.7
58358	Dongshan	31.07	120.43	17.5
58367	Xujiahui	31.17	121.43	2.6
58457	Hangzhou	30.23	120.17	41.7
58464	Pinghu	30.62	121.08	5.4
58549	Jinhua	29.12	119.65	62.6
58556	Shengzhou	29.60	120.82	104.3
58562	Yinxian	29.87	121.57	4.8
58633	Quzhou	29.00	118.90	82.4
58646	Lishui	28.45	119.92	59.7
58647	Longquan	28.07	119.13	195.5
58659	Wenzhou	28.03	120.65	28.3
58665	Hongjia	28.62	121.42	4.6

$$S = \mathrm{sgn}(x_j - x_i) = \begin{cases} 1, & x_j > x_i \\ 0, & x_j = x_i \\ -1, & x_j < x_i \end{cases} \quad (1)$$

It has been documented that when $n \geq 8$, the statistic S is approximately normally distributed with the mean, and $E(S) = 0$ (Mann 1945; Kendall 1975). The variance statistic is expressed as:

$$\mathrm{Var}(S) = \frac{n(n-1)(2n+5) - \sum_{i=0}^{m} t_i(t_i-1)(2t_i+5)}{18} \quad (2)$$

where m is the number of tied groups, each with t_i tied observations.

The significance of trends can be tested by comparing the standardized variable u in Eq. (3) with the standard normal variate at the desired significance level α (Kendall 1975).

Table 2 Definitions of precipitation indices used in this study

Indices	Definitions	Units
RR	Annual total precipitation amount	mm
RX1day	Annual maximum precipitation amount for 1-day intervals	mm
R25mmT	Annual total precipitation amount with 50 mm/day>precipitation≥25 mm/day	mm
R50mmT	Annual total precipitation amount with precipitation≥50 mm/day	mm
RR1	Annual number of days with precipitation≥1 mm/day	days
R25mm	Annual number of days with 50 mm/day>precipitation≥25 mm/day	days
R50mm	Annual number of days with precipitation≥50 mm/day	days
SDII	Annual simple precipitation intensity (RR/RR1)	mm/d
PCI	Annual precipitation centralization index calculated by day and month [i.e., PCI(day), PCI(month)], respectively	None
R25mmTOT	Percentage of R25mmT to RR	%
R50mmTOT	Percentage of R50mmT to RR	%

$$u(S) = \begin{cases} \dfrac{S-1}{\sqrt{\mathrm{Var(s)}}}, & S > 0 \\ 0, & S = 0 \\ \dfrac{S+1}{\sqrt{\mathrm{Var(s)}}}, & S < 0 \end{cases} \quad (3)$$

A positive (negative) value of $u(S)$ signifies upward (downward) trend. The significance level α is normally set quite low at values of 0.1, 0.05, or 0.01. In this study, trends of precipitation are estimated by the linear regression, while the Mann–Kendall test is employed to determine whether the slope of the regression line is significant. The significance level (α) of 0.05 and 0.01, i.e., confidence level ($1-\alpha$) of 95 and 99 % is used for trend analysis over the YRD region.

3.2.2 Mann–Kendall test of abrupt changes

Time series data points are presumed to be steady, and elements in the series are random and independent from each other. Time series of variables (i.e., $X=\{x_1, x_2, \ldots, x_n\}$) experience no change due to the null hypothesis assuming no trend in data exists. For each data point x_i, n_i is computed by the number of data points that occur later in the series and whose values exceed x_i. The Mann–Kendall statistic n_i is calculated as (Wei 2008; Liang et al. 2011; Jones et al. 2015):

$$d_k = \sum_{i=1}^{k} n_i, \quad 2 \le k \le n \quad (4)$$

Under the null hypothesis where no trend is assumed, the statistic d_k is distributed as a Gaussian distribution with an expected value of $E(d_k)$ and a variance of $\mathrm{Var}(d_k)$ as follows:

$$E(d_k) = \frac{k(k-1)}{4}, \quad 2 \le k \le n \quad (5)$$

$$\mathrm{Var}(d_k) = \frac{k(k-1)(2k+5)}{72}, \quad 2 \le k \le n \quad (6)$$

The standard value of d_k is computed by:

$$u(d_k) = \frac{d_k - E(d_k)}{\sqrt{\mathrm{Var}(d_k)}}, \quad 2 \le k \le n \quad (7)$$

This is the forward sequence. Given that $u(d_1)=0$, all $u(d_k)$ will result in a curve UF. In order to search an abrupt change, it is necessary to perform a similar analysis on the reverse time series. A retrograde $u\,(d_k)$ is expressed in Eq. (8).

$$u'(d_k) = -u(d_{k'}) \quad k' = n+1-k, \quad 2 \le k \le n \quad (8)$$

Given that $u\,(d_1)=0$, all $u\,(d_k)$ will establish a curve UB. The intersection point of UF and UB located between the confidence lines is the time when climate jump occurs. A typical confidence level of 95 % is used in the detection of the precipitation series (Liang et al. 2011).

3.3 Morlet wavelet analysis

The Morlet wavelet analysis is employed to analyze the periodicity of precipitation. The wavelet analysis results in a series of wavelet coefficients, which indicate how close the signal is to the particular wavelet. The corresponding wavelet family consists of a series of sub-wavelets, which is generated by dilation and translation operations from the basic wavelet function $\psi(t)$ shown as follows (Zhang et al. 2008; Zhu et al. 2009; Liu and Tang 2011):

$$\psi_{a,b}(t) = |a|^{-\frac{1}{2}} \psi\left(\frac{t-b}{a}\right) a, b \in \mathrm{R}, a \neq 0 \quad (9)$$

where $\psi_{a,b}(t)$ is the sub-wavelet, and parameters a and b denote the scale factor and the horizontal shift, respectively.

For any function $f(t) \in L^2(R)$, its WT is expressed as:

$$W_f(a,b) = |a|^{-\frac{1}{2}} \int_{-\infty}^{+\infty} \mathrm{f}(t) \psi^*\left(\frac{t-b}{a}\right) \mathrm{d}t \quad (10)$$

where $W_f(a,b)$ is wavelet coefficient, and asterisk denotes the conjugate.

Based on the wavelet coefficient, the wavelet variance, which is used to determine the main cycles and its signal strength, is computed according to the following Eq. (11).

$$\mathrm{Var}(a) = \int_{-\infty}^{+\infty} \left|W_f(a,b)\right|^2 \mathrm{d}b \quad (11)$$

Using the Morlet wavelet analysis, the original signal or series is decomposed on a time-scale plane. Therefore, the local character in the time–frequency field can be clearly studied, and significant periodicity in the signal or series can be distinguished.

4 Results and discussion

4.1 Changes of the general precipitation

Figure 2 shows the spatial distribution of annual average values of the general precipitation indices over the YRD region during 1960–2012. The mean magnitude of the precipitation indices vary markedly throughout the YRD region, as a consequence of the climatic heterogeneity of the study area. There is a marked decreasing gradient in RR, from more than 1600 mm in the southeastern mountains and coasts to <850 mm in the northern plains of the study area (Fig. 2a). The spatial distribution of RX1day shows that the lowest values (RX1day<80 mm) occur in the central parts of the study area, whereas the highest values (RX1day>130 mm) are found along the southeastern coasts and in the north corner of the study area (Fig. 2b). RR1 ranges from about 60 days to

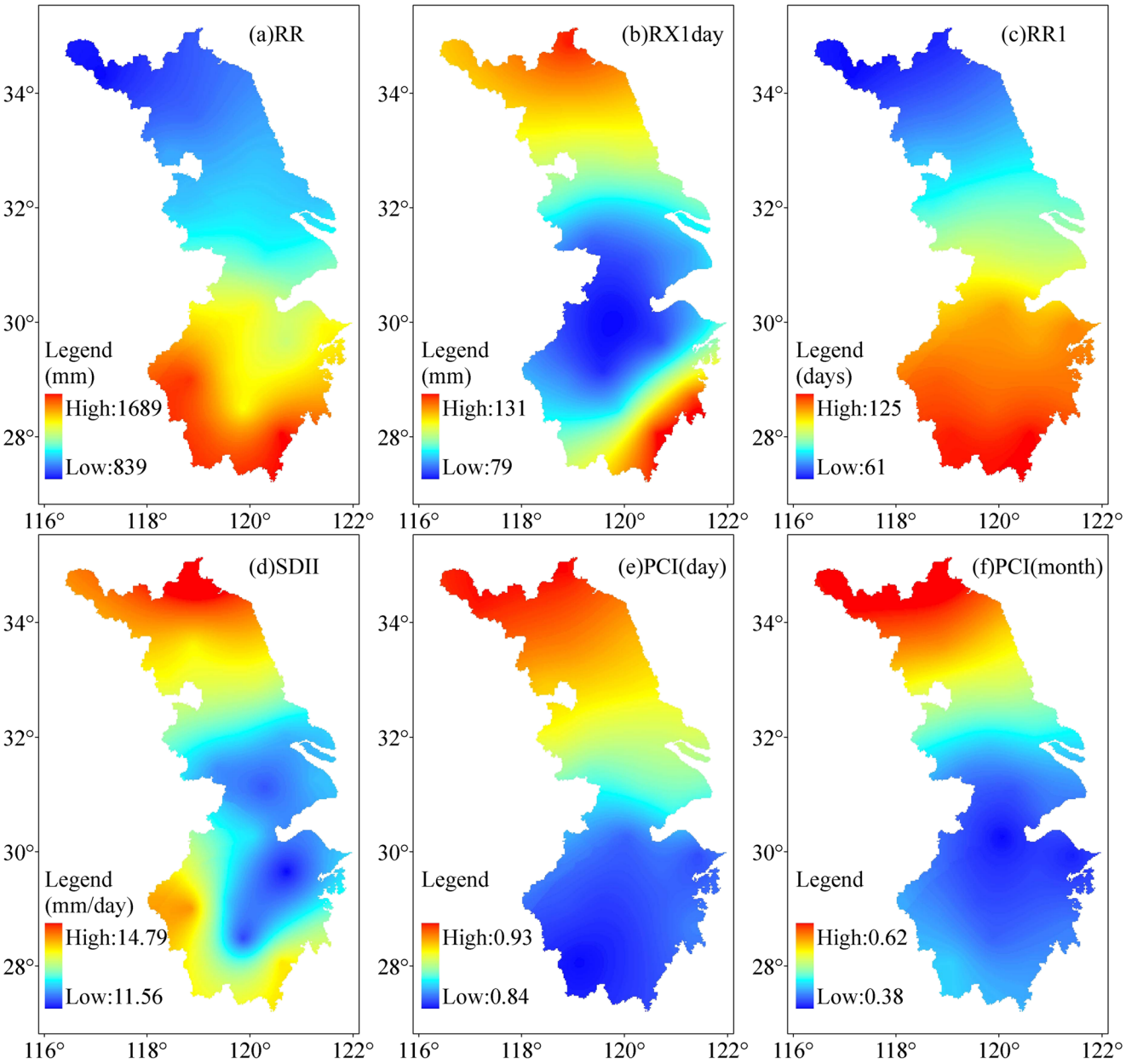

Fig. 2 Spatial distribution of annual average values of the general precipitation indices over the YRD region during 1960–2012

more than 120 days, and an obvious increasing trend in this index is apparent along the northwest–southeast section (Fig. 2c). The spatial distribution of SDII is similar to those observed for RX1day, with the lowest intensities (SDII<12 mm/day) in the central units of the study area (Fig. 2d). However, unlike RX1day values, the highest intensities of SDII (SDII>14 mm/day) appear only in the northern part of the study area. The PCI values, calculated using the daily and monthly precipitation according to the method of Xu (2006), gradually reduces from 0.931 to 0.840 [PCI(day)] and from 0.617 to 0.380 [PCI(month)] (Fig. 2e, f), respectively. Meanwhile, clear negative trend can be detected both in PCI(day) and PCI(month) values along the northwest–southeast section, which coincided with that of RR in the opposite.

Consequently, it can be concluded that there is more precipitation in the southeast area than that in the northwest area, and the daily and monthly distributions of the precipitation in the southeast area are more homogeneous than that of the precipitation in the northwest area.

Figure 3 shows the annual evolution (normalized and smoothed series) and temporal trends for the general precipitation over the YRD region during 1960–2012. Table 3 shows the trends per decade and number of stations with positive/negative trends for areal mean precipitation over the YRD region during 1960–2012. Figure 4 shows the spatial patterns

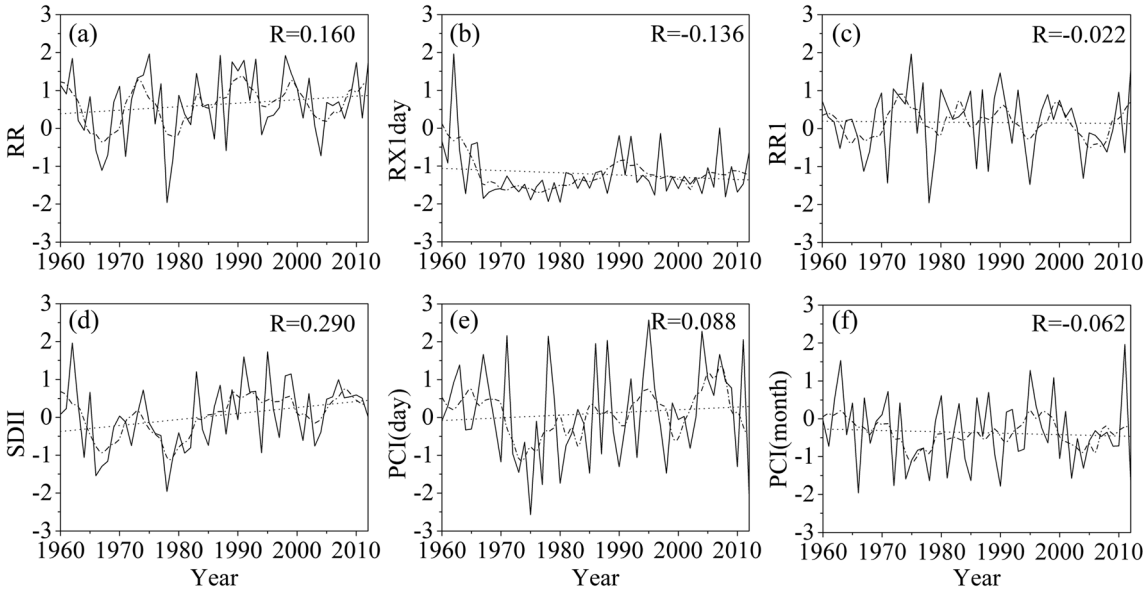

Fig. 3 Annual evolution (normalized and smoothed series) and temporal trends for the general precipitation indices over the YRD region during 1960–2012

of trends per decade for the general precipitation indices over the YRD region during 1960–2012. The RR exhibits a slight increasing trend of 14.78 mm/decade over the period 1960–2012, with a range from −25.61 to 49.79 mm/decade (Fig. 3a, Table 3), which increases significantly throughout most parts of the study area with the north being an exception (Fig. 4a). Nineteen stations show insignificant rising trends, distributed mainly in the central and southern parts of the study area (Table 3, Fig. 4a). The other five stations exhibit insignificant declining trends, which are mainly located in the north of the study area (Table 3, Fig. 4a). The RX1day shows a decreasing trend, and the regional trend at the mean rate of −1.26 mm/decade with a range from −5.37 to 11.79 mm/decade (Table 3, Fig. 3b). Ten stations have negative trends, while 14 stations show obvious positive trends, among which only two stations (i.e., Jinhua and Hongjia) are statistically significant under 5 % level (Fig. 4b). Unlike RR, the spatial distribution of RX1day is very scattered (Fig. 4b), and the RX1day in the mid-south of the study area has stronger trends than that in the north. For RR1, there is no obvious decreasing tendency with the slope of the regression line being −0.12 days/decade (Table 3, Fig. 3c). Fourteen stations show decreasing trends, distributed in the north and south of the study area. However, ten stations exhibit increasing trends, locating in the central parts of the study area (Table 3, Fig. 4c), and the RR1 of the central parts is apparently more than that of the southern and northern parts. Meanwhile, none of these stations is significant at the 95 % confidence level.

Table 3 Trends per decade and number of stations with positive or negative trends for regional precipitation over the YRD region during 1960–2012

Indices	Regional trends	Range	Units	Number of stations showing positive trend	Number of stations showing negative trend
RR	14.78	−25.61 to 49.79	mm/decade	19 (0)	5 (0)
RX1day	−1.26	−5.37 to 11.79	mm/decade	14 (2)	10 (0)
RR1	−0.12	−1.75 to 1.51	days/decade	10 (0)	14 (0)
SDII	0.17	−0.21 to 0.46	mm/day/decade	21 (1)	3 (0)
PCI(day)	0.0006	−0.0009 to 0.003	None	18 (1)	6 (0)
PCI(month)	−0.002	−0.011 to 0.009	None	10 (0)	14 (0)
R25mm	0.17	−0.52 to 0.80	days/decade	18 (2)	6 (1)
R50mm	0.10	−0.29 to 0.38	days/decade	20 (1)	4 (0)
R25mmT	6.14	−16.83 to 27.67	mm/decade	19 (1)	5 (1)
R50mmT	7.31	−22.46 to 27.09	mm/decade	20 (0)	4 (0)
R25mmTOT	0.16	−1.90 to 1.20	%/decade	13 (0)	11 (1)
R50mmTOT	0.44	−1.40 to 1.87	%/decade	18 (0)	6 (0)

The number in brackets represents the counts of stations with statistically significant trends at the 5 % level

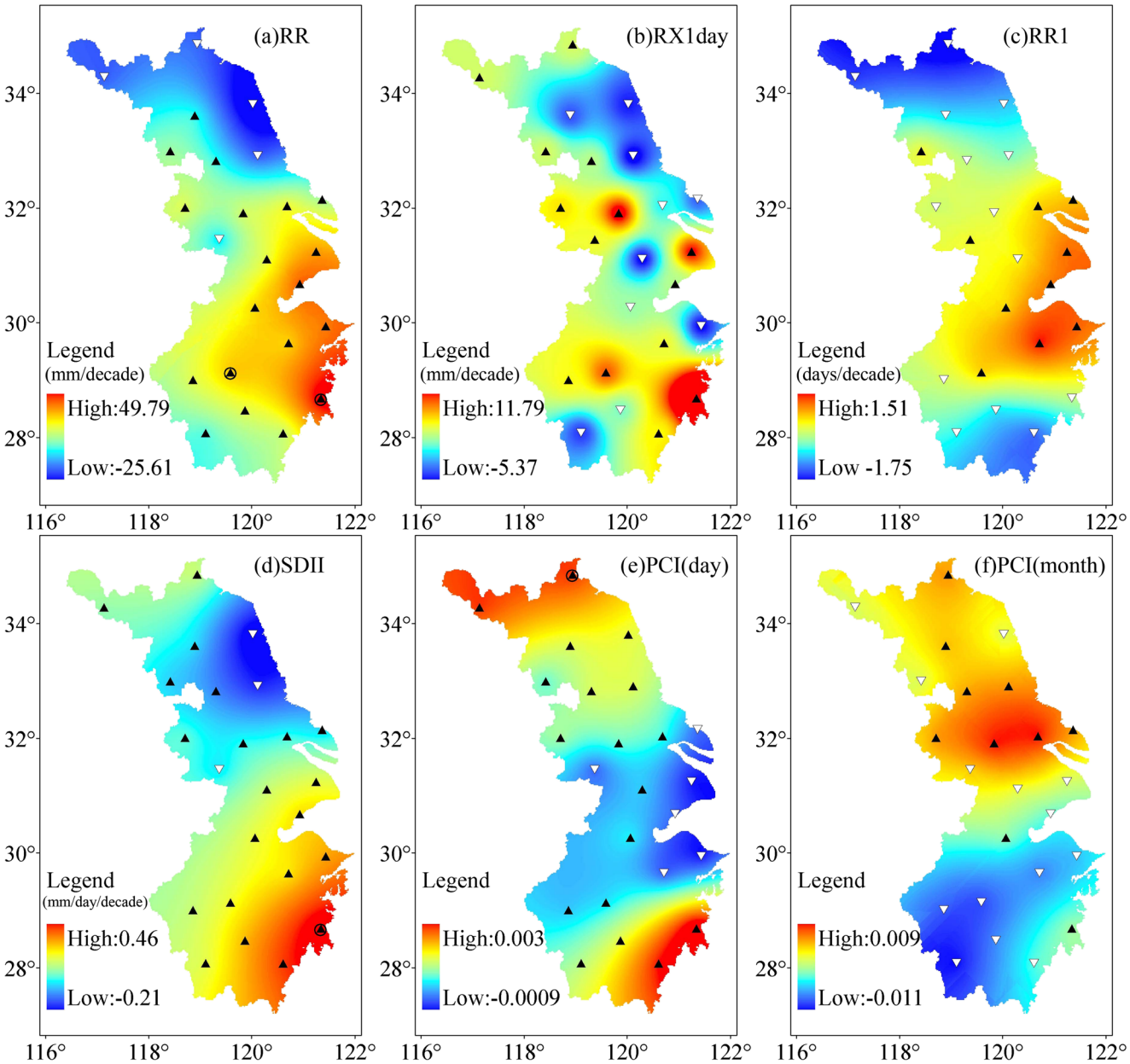

Fig. 4 Spatial patterns of trends per decade for the general precipitation indices over the YRD region during 1960–2012. *Black triangles* denote increasing trends, *white triangles* denote decreasing trends, and *triangles with circles* show significant trends at the 95 % confidence level

Increasing RR and decreasing RR1 result in increasing SDII. Consequently, a remarkable increasing trend of SDII can be seen across most of the stations, and with a regional rate of 0.17 mm/decade ranging from −0.21 to 0.46 mm/decade, although only the Hongjia station has statistically significant positive trend. The other three stations (i.e., Sheyang, Dongtai, and Liyang) show negative trends (Table 3, Fig. 3d). The highest positive trends appear in the southern coastal regions, while the lowest negative trends appear in the northern coastal regions (Fig. 4d). As shown in Table 3 and Fig. 3e and f, the indexes of PCI(day) and PCI(month) have the opposite trends. As for PCI(day), 18 stations show positive trends, while 6 stations show negative trends. Ganyu station exhibits statistically significant positive trend among the 24 stations. But for PCI(month), 14 stations show increasing trends, while 10 stations show decreasing trends. Except for the southeastern coastal regions, the mean rates of PCI(day) trend and PCI(month) trend gradually increase from the southeast to the northwest of the study area (Fig. 4e, f).

In summary, the central and southern parts of the study area have become more humid than the northern part of the study area, and the monthly precipitation tends to be

more homogeneous in the YRD region since 1960 with exception of the north parts. However, the daily precipitation has undergone a consistent concentrated trend over almost all of the study area since 1960, implying the enhanced possibility of extreme precipitation (i.e., heavy precipitation or drought). A strengthening in the precipitation intensity and a reduction in the rainfall frequency are found over the urban areas, especially in the central regions. Meanwhile, the increment of RX1day is more obvious in the rapid urbanization area to a certain degree in the YRD region than that in the slow urbanization, implying that RX1day is likely to be related to the urbanization produces.

4.2 Changes of the heavy precipitation

Figure 5 shows the spatial distribution of annual average values of the heavy precipitation indices over the YRD region during 1960–2012. R25mm ranges from 6.23 to 13.94 days. There is a marked increasing gradient from the northwest to southeast, and the maximum value appears in the western mountain area of Zhejiang province, whereas the minimum value is located at the northernmost corner (Fig. 5a). The spatial distributions of R25mmT and R25mmTOT are similar to that of R25mm, and with a range from 212.79 to 478.51 mm and from 22.89 to 28.99 %, respectively (Fig. 5b, c). As for R50mm, R50mmT, and R50mmTOT, there

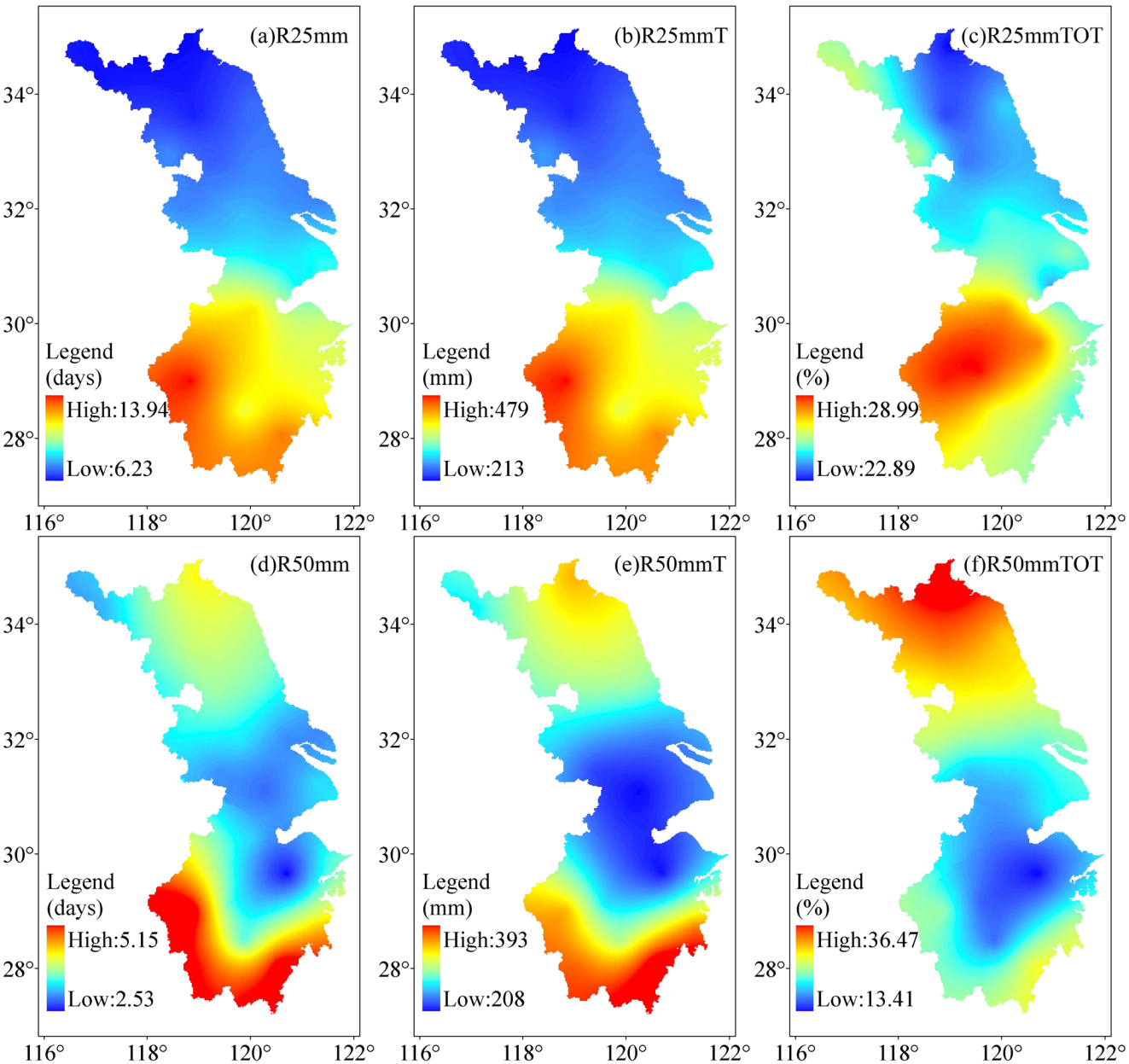

Fig. 5 Spatial distribution of annual average values for the heavy precipitation indices over the YRD region during 1960–2012

are nearly consistent features of spatial distributions, with the high values in the north or south, while the low values are observed in the middle of the study area (Fig. 5d–f). Among the three indices, R50mm ranges from 2.53 to 5.15 days, with extreme located in the western mountain area of Zhejiang province (Fig. 5d); R50mmT ranges from 207.82 to 392.84 mm, with extreme values along the southeastern coastal region (Fig. 5e); R50mmTOT ranges from 13.41 to 36.47 %, which extreme values are detected in the northern coastal region of the study area (Fig. 5f).

Based on the above analysis, it is found that though the frequency of heavy precipitation in the northwest is lower than that of the southeast of the study area, the contribution of the torrential rain to total precipitation in the northwest of the study area is higher than that of the southeast, which tends to produce the extreme events, especially the droughts and floods.

Figure 6 shows the annual evolution (normalized and smoothed series) and temporal trends for the heavy precipitation indices over the YRD region during 1960–2012. Figure 7 shows the spatial patterns of trends per decade for the heavy precipitation indices over the YRD region during 1960–2012. The R25mm indicates an increasing trend in the past decades, at the average rate of 0.17 day/decade (Table 3, Fig. 6a). Increasing R25mm can be found at 18 stations over the study area, and these stations are located mainly in the mid-south YRD region (Fig. 7a). Among these stations, the increasing trends of two stations (i.e., Hongjia and Yinxian) are statistically significant at the 95 % confidence level, which are concentrated in the southeast coastal region of the study area. However, there are six stations with decreasing trends, and only one Ganyu station shows a statistically significant trend (Fig. 7a). The R25mmT also exhibits an increasing trend, and the regional trend is at the rate of 6.14 mm/decade with a range from −16.83 to 27.67 mm/decade (Table 3, Fig. 6b). Meanwhile, 19 stations show positive trends, while 5 stations exhibit negative trends. Furthermore, two stations (i.e., Hongjia and Ganyu) are statistically significant. The spatial distribution of R25mmT trends is similar to that of R25mm (Fig. 7b). As for R25mmTOT, there is a weak increasing trend with the mean rate of 0.16 %/decade (Table 3, Fig. 6c). Increasing R25mmTOT and decreasing R25mmTOT can be observed at 13 and 11 stations, respectively (Fig. 7c). Among all of these stations, only one station (Ganyu) has statistically significant negative trend. The spatial distribution of R25mmTOT trends is likewise similar to that of R25mm (Fig. 7c).

But for R50mm, there is a positive tendency with remarkable fluctuations during the study period (Fig. 6d). It can be seen from Fig. 7d that there are 20 stations being characterized by increasing R50mm at the mean rate of 0.1 day/decade, and these stations are distributed mainly in the middle and southern parts of the study area, especially the Gulf of Hangzhou (Table 3, Fig. 7d). Among these stations, the Pinghu station is statistically significant with increasing R50mm, which is located in the north of the Gulf of Hangzhou (Fig. 7d). Accordingly, there are only four stations with the decreasing R50mm (Fig. 7d). In this sense, the YRD region is dominated by increasing R50mm in general. As for R50mmT, there is a positive trend during the study period 1960–2012 (Fig. 6e), with a

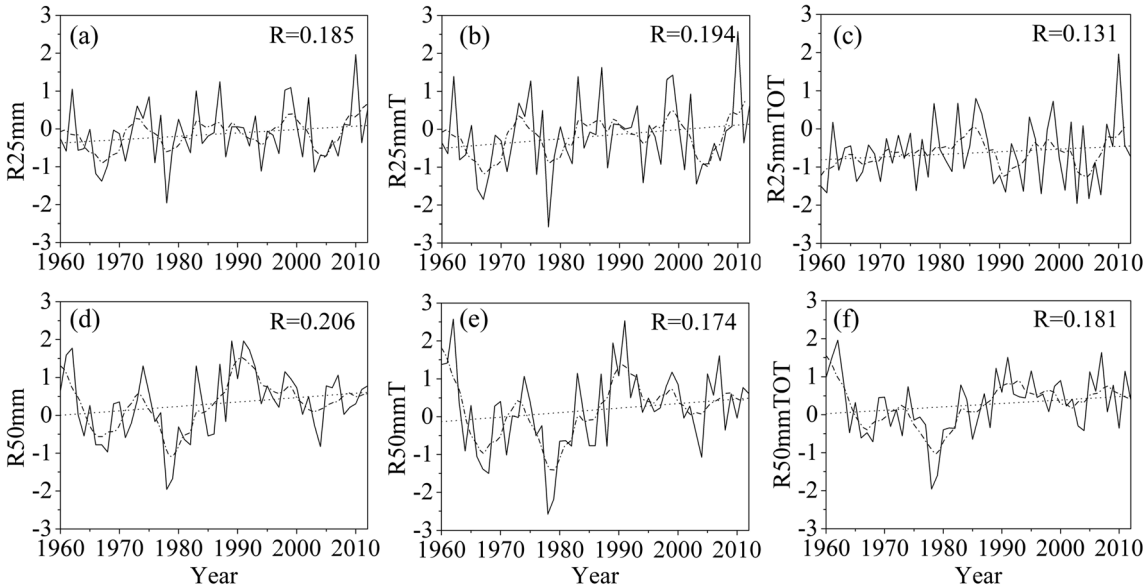

Fig. 6 Annual evolution (normalized and smoothed series) and temporal trends for the heavy precipitation indices over the YRD region during 1960–2012

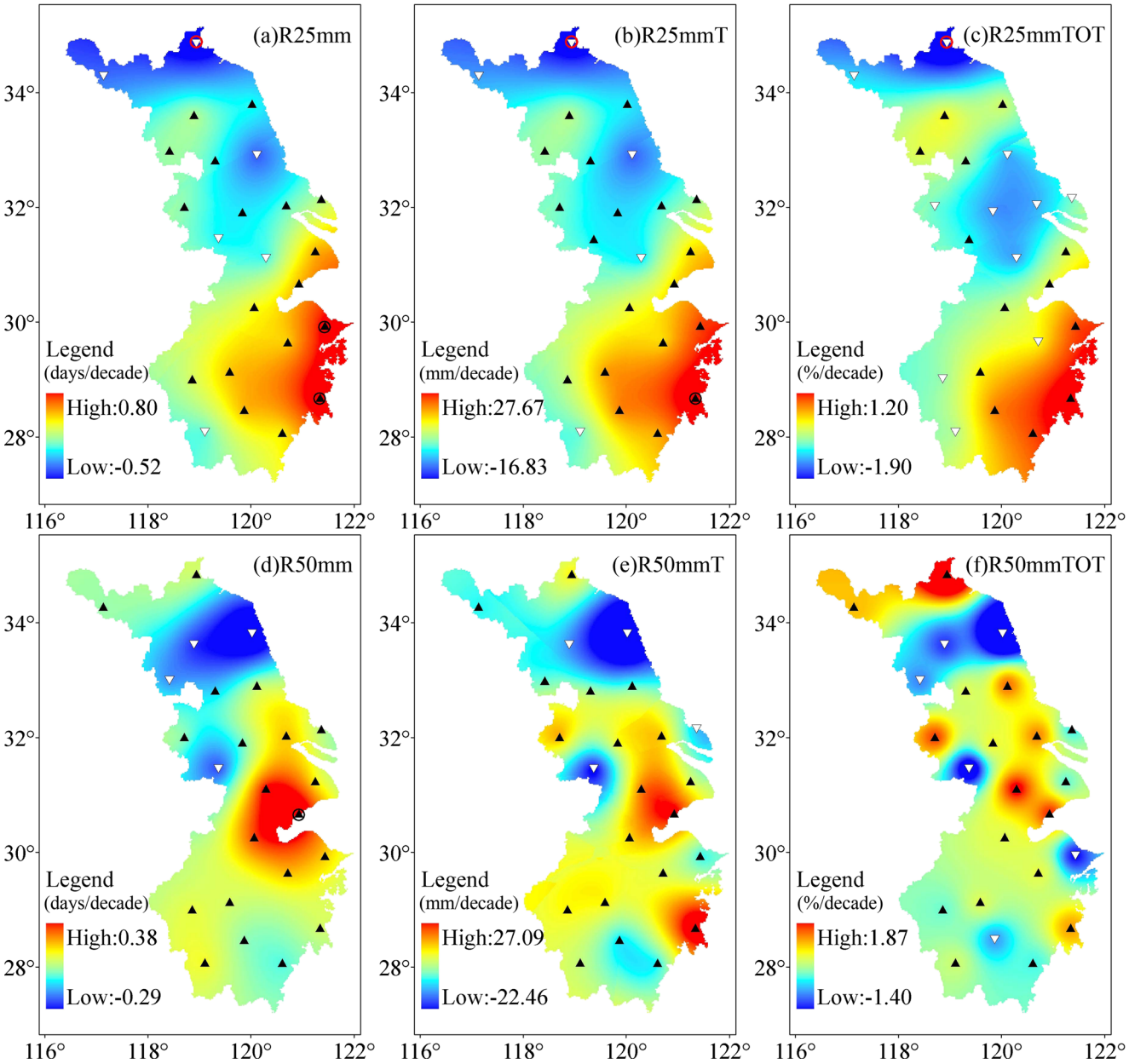

Fig. 7 Spatial patterns of trends per decade for the heavy precipitation indices over the YRD region during 1960–2012. *Black triangles* denote increasing trends, *white triangles* denote decreasing trends, and *triangles with circles* show significant trends at the 95 % confidence level

regional rate of 7.31 mm/decade (Table 3). Increasing R50mmT and decreasing R50mmT can also be detected at 20 stations and 4 stations, respectively (Table 3). The spatial distribution of R50mmT trends is similar to that of R50mm, which indicates that a large proportion of increasing stations are located in the central and southern YRD region (Fig. 7e). As for R50mmTOT, a slight positive trend can be found for R50mmTOT with the average rate of 0.44 %/decade (Table 3, Fig. 6f). However, increasing R50mmTOT and decreasing R50mmTOT are shown in 18 and 6 stations, respectively (Fig. 7f). The spatial distribution of R50mmTOT trends is also similar to that of R50mm, while the north corner of the study area has highest increasing trends, although the mid-south of the study area still increase strikingly.

As a consequence, the above analysis suggests that the frequency and contribution of the heavy precipitation (especially the torrential rain) have arisen dramatically in almost all of the study area since 1960, and the precipitation event has showed an obvious trend of extremeness, agreeing with the studies in Beijing (Song et al. 2014; Zhang et al. 2014) and the value of PCI. If the precipitation trend occurred remains unchanged, the future of the YRD region might have to face with more storms and floods, and the damage caused by the heavy precipitation might be more serious.

4.3 Correlation coefficients of precipitation indices

The correlations between the precipitation indices are shown in Fig. 8 and tested under the 99 % confidence level, which is in accordance with the previous study (Cao and Pan 2014). The results indicate that the heavy precipitation indices (i.e., R25mm, R50mm, R25mmT, R50mmT, and R50mmTOT) have high correlations with the annual total precipitation (RR), and increases/decreases in the heavy precipitation can result in the increase/decrease in the annual total precipitation to some extent. The correlation coefficients among them are 0.83, 0.81, 0.84, 0.81, and 0.59, respectively (Fig. 8e–i), and also statistically significant at the 0.01 significance level, which show that RR is well correlated with the heavy precipitation. Actually, the heavy precipitation contributes more than 90 % of the increase in precipitation over the YRD region during 1960–2012 (Table 3). Meanwhile, the correlations coefficients between RR and RR1, SDII, and PCI(day) are likewise significant at the 99 % confidence level(Fig. 8b–d), indicating that the rainfall has been much concentrated and extreme in the YRD region during the study period. However, the correlation coefficients between RR and RX1day (Fig. 8a), PCI(month), and R25mmTOT are <0.30 and likewise statistically nonsignificant at the 0.01 level, which show that the correlations between them are not obvious, and changes in RX1day, PCI(month), and R25mmTOT have little or indirect impacts on RR over the YRD region during the study period.

4.4 Abrupt changes of precipitation

Figure 9 shows the sequential Mann–Kendall analysis results for RR, RX1day, SDII, R50mm, R50mmT, and R50mmTOT over the YRD region during 1960–2012. The UF curve of RR indicates a decreasing trend from 1960 to 1988 except the middle 1970s, while an increasing trend is found during 1989–2012. The increasing variation in RR is obvious before 2002, and after that, RR decreases gradually (Fig. 9a). For RX1day, the UF curve is under zero for most of the period, and it intersects with the critical value lines for a short period, which confirms a decreasing trend especially before 1990 (Fig. 9b). The UF curve of SDII shows a decreasing trend from 1960 to 1989, while opposite trend is found during the period 1990–2012. There is an obvious increasing tendency in SDII since 1990, which is significant during the period 2009–2012 as the values of UF exceeds the critical limit (Fig. 9c). As shown in Fig. 8d and f, the UF curves of R50mm, R50mmT, and R50mmTOT present the synchronous trends to a certain extent, and these UF curves exhibit decreasing trends before 1990, and after that, there are marked increasing trends (Fig. 9d–f).

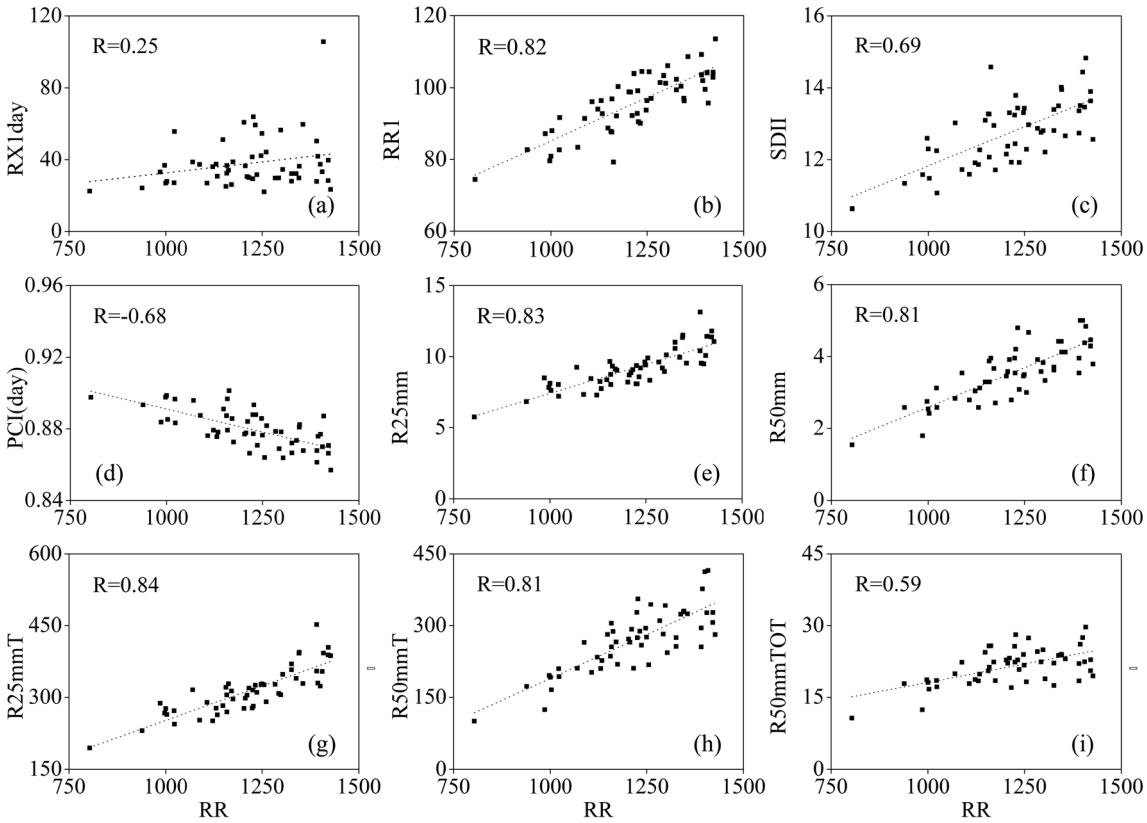

Fig. 8 Correlations between the precipitation indices over the YRD region during 1960–2012

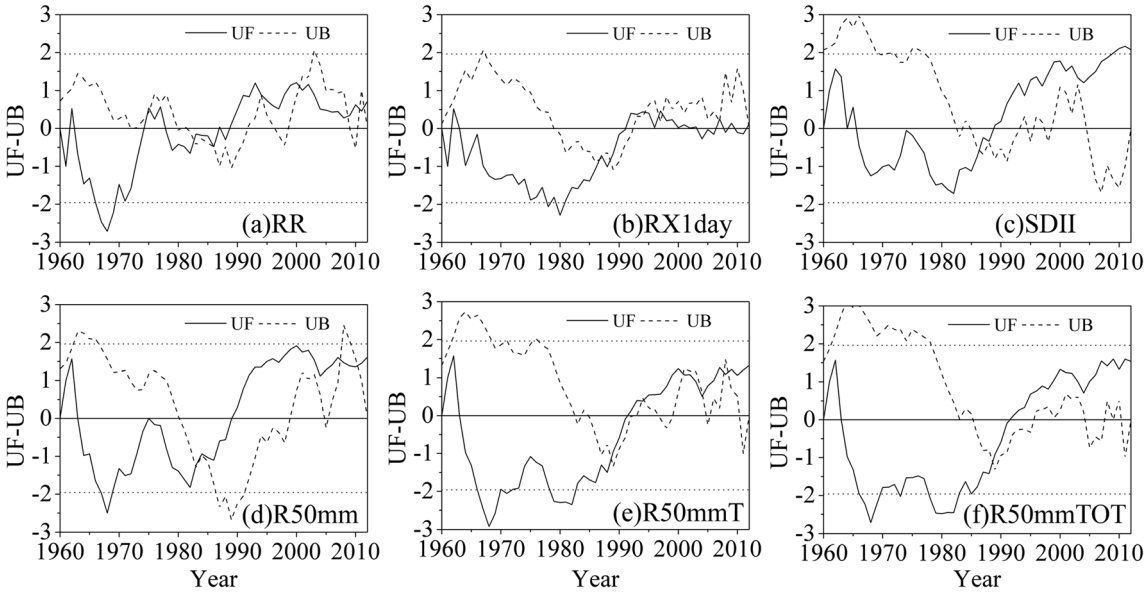

Fig. 9 Sequential Mann–Kendall analysis results for RR (**a**), RX1day (**b**), SDII (**c**), R50mm (**d**), R50mmT (**e**), and R50mmTOT (**f**) over the YRD region during 1960–2012. The *horizontal dashed line* represents the critical value at the 5 % significance level

As for these indices, only one main abrupt change point (at 5 % significance level) is detected as the intersection point of the two curves (i.e., UF and UB curves) located with the confidence interval during the study period 1960–2012, and the abrupt increasing step changes occur in 1984, 1988, 1987, 1984, 1988, and 1988, respectively (Fig. 9). Consequently, the results of change point analysis indicate that almost all of these changes have similar start time, and the abrupt change of precipitation occurred consistently in the mid-1980s over the YRD region, and after then, the precipitation increased significantly, which is similar with the previous studies in other areas (Shi and Xu 2008; Lv et al. 2009; Chi et al. 2013). Furthermore, it is worth mentioning that the torrential rain develops and changes with the synchronization of the annual total precipitation over the YRD region during the study period.

4.5 Periodicity analysis of precipitation

Figure 10 shows the real part of the wavelet transform and the wavelet variances of RR, RR1, SDII, R50mm, and R50mmTOT over the YRD region during 1960–2012. Figure 10a and b shows that there are three main cycles of RR: 4–6-year cycle, 12–14-year cycle, and 19–21-year cycle. The 4–6-year cycle appears mainly in the mid-1960s, 1980s, and the early twenty-first century, while the 12–14-year cycle dominates the period from 1980 to 2000. Interdecadal cycle of 19–21 years exists notably before the 1980s. Figure 10c and d indicates that there are also three main cycles of RR1: 4–7-year cycle, 12–14-year cycle, and 19–21-year cycle. Among these cycles, the 4–7-year cycle almost arises throughout the time sequence, and the 12–14-year cycle exists in the period from the late 1970s to the early 1990s. Unlike RR, the 19–21-year cycle of RR1 dominates the entire study period. As shown in Fig. 10e and f, there are two main change cycles and one unremarkable cycle in index SDII: 5–6-year cycle, 19–21-year cycle, and 13-year cycle. The 5–6-year cycle appears in the 1960s and the period from 1980 to 2005, while the 19–21-year cycle is also observed steadily in the period 1960–1980. The unremarkable 13-year cycle appears after the mid-1980s. It can be discovered that three main cycles of 5–6 years, 11–13 years, and 20–23 years exist in the index R50mm over the study period (Fig. 10g, h). The 5–6-year cycle exists in the 1960s and the early 1980s, but the 11–13-year cycle is evident after the late 1970s, and that, the 20–23-year cycle is likewise detected in the period 1960–1980. As shown in Fig. 10i and j, the change period of R50mmTOT have 5–6-year cycle, 9–13-year cycle, and 18–20-year cycle. The 5–6-year cycle exists in the early 1960s and the early 1980s, while the 11–13-year cycle and 18–22-year cycle are visible during the period 1970–2012 and 1960–1980, respectively. In addition, there is still a nonsignificant 2-year cycle in these indices throughout the entire study period, though the signal is very weak (Fig. 10), which might represent the quasi-biennial oscillation of summer monsoon rainfall in Eastern China (Huang et al. 2006; Jia et al. 2009).

Based on the foregoing periodicity analysis, it is concluded that three main change cycles and one weak cycle are coexisted over the YRD region in the study period 1960–2012, namely, 5–6-year cycle, 13-, 20-, and 2-year cycle. Furthermore, it is clear that the significant change of cycles occurred in the 1980s when the short cycle was set to overtake the long cycle, which is almost concordant with the above studies of abrupt change of precipitation, leading to high frequency and instability of precipitation changes over the YRD region in recent decades.

4.6 Cause of precipitation changes

In the background of global warming, the climate has changed obviously in the Yangtze River Delta (Jiang et al. 2009), especially the precipitation increasing significantly. There might be three main factors that have effects on the precipitation in the YRD region, namely, global warming, change of East Asian summer monsoon, and urbanization development.

First is global warming: Over the twentieth century, especially since the 1990s, continuously increasing concentration of atmospheric carbon dioxide is resulting in global warming. Global warming is likely to have significant effects on the hydrological cycle (IPCC 2007), which speeds up global water cycle and strengthens evaporation, moisture, and rainfall. Furthermore, an important consequence of global warming is an increase in the magnitude and frequency of extreme precipitation events generated by increased atmospheric moisture levels, thunderstorm activity, and/or large-scale storm activity (Roy and Balling 2004). Most climate models also project increases in precipitation extremes as the climate warms (Tebaldi et al. 2006; O'Gorman and Schneider 2009). Therefore, global warming is the background factor that influences the frequency and volume of the precipitation in the YRD region during 1960–2012.

Second is the change of East Asian summer monsoon: The YRD region is controlled by the East Asian monsoon (Svensson 1999), the advance and retreat of East Asian summer monsoon determine to a large extent the timing of the rainy season and the amount of rainfall, and the position of the summer belt is southward (northward) of its mean when East Asian summer monsoon is weak (strong). As for the middle and lower reaches of the Yangtze River, the East Asian summer monsoon is negatively (positively) correlated with summer rainfall (Yang et al. 2013), and the flooding (drought) years are related to the weak (strong) monsoon (Shi et al. 1996). At the end of the 1970s, a jump of the monsoon intensity occurred, and simultaneously, the monsoon in summer weakened significantly. Meanwhile, the precipitation mainly concentrated in the Yangtze River Valley from then on (Jiang et al. 2006), which is in line with the changes of precipitation in the YRD region during the study period. Therefore, change of East Asian summer monsoon is the key factor that influences the frequency and volume of the precipitation in the YRD region during 1960–2012.

Third is urbanization process: The urban water cycle and the local climatic environment are invariably affected by the urban growth (Foley et al. 2005). The urbanization not only modifies the exchange of heat, water, and momentum between the land surface and overlying atmosphere (Crutzen 2004) but also changes the composition of the atmosphere over urban areas (Pataki et al. 2003). Urbanization-driven land use change influences the local hydrometeorological processes, changes the urban micro-climate, and sometimes affects the precipitation significantly (Pathirana et al. 2014). Controlled experiments verify that there is a significant impact of urban heat island on cumulative rainfall quantities resulting in increases of 10–13 % (Shem and Shepherd 2009). Sensitivity studies, however, show that there is a significant increase in local extreme rainfall when the urban area is increased (Pathirana et al. 2014). In addition, the urbanization signatures in strong precipitation are significantly different from those in weak precipitation over the urban areas (Li et al. 2011). Due to the increasing concentration of businesses and infrastructure, the urbanization process continued at a phenomenal rate over the YRD region in the last decades. With the rapid development of urbanization, the annual precipitation and the flood season precipitation in the urban areas showed a striking increase, and the rapid urbanization has greatly influenced the regional laws of hydrology in the YRD region (Xu et al. 2010). This suggests a possible impact of urbanization on variability of rainfall for the region. Therefore, the urbanization process is the local factor that influences the frequency and volume of the precipitation in the YRD region during 1960–2012.

Fig. 10 Real part of the wavelet transform (**a**, **c**, **e**, **g**, **i**) and the wavelet variances (**b**, **d**, **f**, **h**, **j**) of RR, RR1, SDII, R50mm, and R50mmTOT over the YRD region during 1960–2012

5 Conclusions

In this study, the long-term trends of daily precipitation of 24 stations are analyzed over the YRD region during the period 1960–2012, using 12 precipitation indices. According to the above analysis, the main conclusions are summarized as follows:

1. For the regional average trends of precipitation over the YRD region during the study period, with PCI(day) arising weakly, the indices of RR, R25mmT, R50mmT, R25mm, R50mm, SDII, R25mmTOT, and R50mmTOT increase at the rates of 14.78, 6.14, 7.31 mm/decade, 0.17, 0.10 days/decade, 0.17 mm/day/decade, 0.16, and 0.44 %/decade, respectively. On the contrary, with PCI(month) decreasing indistinctively, RX1day and TWD display decreasing trends, and at the rates of −1.26 mm/decade and −0.12 days/decade, respectively.
2. The central and southern parts of the study area have become more humid than the northern part of the study area during 1960–2012, and the monthly precipitation tends to be more homogeneous with exception of the north area. The daily precipitation has undergone a consistent concentrated trend over almost all of the study area since 1960, implying the enhanced possibility of extreme precipitation (i.e., heavy precipitation or drought). What is more, the frequency and contribution of the heavy

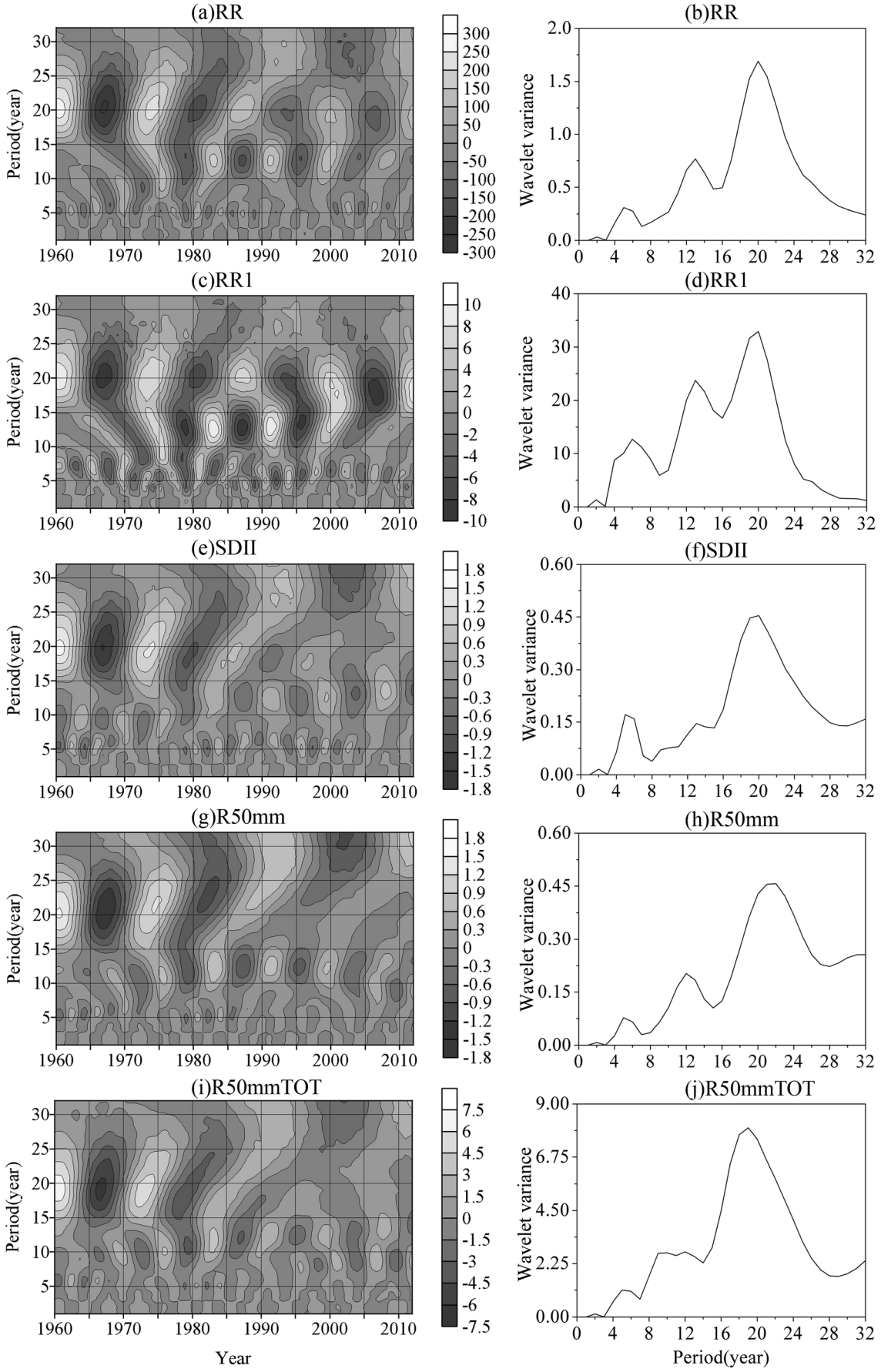
(a)RR
(b)RR
(c)RR1
(d)RR1
(e)SDII
(f)SDII
(g)R50mm
(h)R50mm
(i)R50mmTOT
(j)R50mmTOT
Period(year)
Wavelet variance
Year
Period(year)

precipitation have also arisen dramatically in almost the entire YRD region since 1960, and the precipitation event has showed an obvious trend of extremeness.

3. The annual total precipitation is correlated strongly with most of the other precipitation indices, especially the heavy precipitation indices, which are responsible for more than 90 % of the increment of precipitation. Moreover, the correlations between the precipitation indices indicate that the rainfall has been much concentrated and extreme over YRD region during the study period.
4. Abrupt changes for RR, RX1day, SDII, R50mm, R50mmT, and R50mmTOT are detected in 1984, 1988, 1987, 1984, 1988, and 1988, respectively. The results of change point analysis indicate that almost all these changes have a similar start time, and the abrupt change of precipitation occurred consistently in the mid-1980s over the YRD region during the study period.
5. Three major cycles of precipitation are 5–6-year cycle, 13-year cycle, and 20-year cycle with apparent periodic oscillation characteristics over the YRD region during the study period, together with a coexisting 2-year nonsignificant cycle. In addition, a significant change of cycles occurred in the 1980s over the YRD region, when the short cycle was set to overtake the long cycle, resulting in high frequency and instability of precipitation changes over the YRD region in recent decades.
6. Three factors, which are the global warming, the East Asian summer monsoon change, and the urbanization development, might have impacts on the precipitation, promoting the increase in precipitation over the YRD region during 1960–2012. Among these factors, the variation of East Asian summer monsoon is the key factor that controls mainly the increase in the precipitation, while the global warming and the urbanization development are the background factor and the local factor, respectively.

Acknowledgments The research is financially supported by the National Natural Science Foundation of China (Grant Nos. 41371046, 41301011, and 41301029), the Water Resources Public-Welfare Program (Grant Nos. 201201072 and 201301075), and the Natural Science Foundation of Jiangsu Province (Grant No. BK20131276). Our cordial gratitude should also be extended to the Editor and two anonymous reviews for their professional and pertinent suggestions and comments, which are greatly helpful for further improvement of the quality of this manuscript.

References

Alexander LV, Zhang X, Peterson TC, Caesar J, Gleason B, Tank AMGK, Haylock M, Collins D, Trewin B, Rahimzadeh F, Tagipour A, Kumar KR, Revadekar J, Griffiths G, Vincent L, Stephenson DB, Burn J, Aguilar E, Brunet M, Taylor M, New M, Zhai P, Rusticucci M, Vazquez-Aguirre JL (2006) Global observed changes in daily climate extremes of temperature and precipitation. J Geophys Res 111:D05109. doi:10.1029/2005JD006290

Altava-Ortiz V, Llasat MC, Ferrari E, Atenciab A, Sirangelo B (2011) Monthly rainfall changes in Central and Western Mediterranean basins, at the end of the 20th and beginning of the 21st centuries. Int J Climatol 31:1943–1958

Altin TB, Barak B (2014) Changes and trends in total yearly precipitation of the Antalya district, Turkey. Soc Behav Sci 120:586–599

Cao L, Pan S (2014) Changes in precipitation extremes over the "Three-River Headwaters" region, hinterland of the Tibetan Plateau, during 1960–2012. Quatern Int 321:105–115

Carrera-Hernández JJ, Gaskin SJ (2007) Spatio temporal analysis of daily precipitation and temperature in the Basin of Mexico. J Hydrol 336(3–4):231–249

Chi Y, Zhang C, Liang C, Wu H (2013) The precipitation change in Eastern Forest regions of China in recent 50 years. Acta Ecol Sin 33:217–226

Crutzen PJ (2004) New directions: the growing urban heat and pollution "island" effect—impact on chemistry and climate. Atmos Environ 38:3539–3540

de Lima MIP, Santo FE, Ramos AM, de Lima JLMP (2013) Recent changes in daily precipitation and surface air temperature extremes in mainland Portugal, in the period 1941–2007. Atmos Res 127: 195–209

Domrös M, Peng G (1988) The climate of China. Spring Verlag Press, New York, p 361

Fatichi S, Caporali E (2009) A comprehensive analysis of changes in precipitation regime in Tuscany. Int J Climatol 29:1883–1893

Foley JA, DeFries R, Asner GP, Barford C, Bonan G, Carpenter SR, Chapin FS, Coe MT, Daily GC, Gibbs HK, Helkowski JH, Holloway T, Howard EA, Kucharik CJ, Monfreda C, Patz JA, Prentice IC, Ramankutty N, Snyder PK (2005) Global consequences of land use. Science 309:570–574

Gaughan AE, Waylen PR (2012) Spatial and temporal precipitation variability in the Okavango–Kwando–Zambezi catchment, southern Africa. J Arid Environ 82:19–30

He S, Zheng Y, Yin J (2013) An analysis on precipitation characteristics over middle and lower reaches of Yangtze River in the last 50 years. Ecol Environ Sci 22(7):1187–1192

Huang R, Chen J, Huang G, Zhang Q (2006) The quasi-biennial oscillation of summer monsoon rainfall in China and its cause. J Atmos Sci 30(4):546–560

IPCC (2007) Climate change 2007: the physical science basis. In: Solomon S, Qin D, Manning M, Chen Z, Marquis M, Averyt KB, Tignor M, Miller HL (eds) Contribution of working Group I to the Fourth assessment report of the Intergovernmental Panel on Climate Change. Cambridge University Press, Cambridge

Jia J, Sun Z, Liu X, Tan G, Xu W (2009) Evolution of summer precipitation Quasi-Biennial Oscillation in Eastern China. J Atmos Sci 33(2):397–407

Jiang Z, He J, Li J, Yang J, Wang J (2006) Northerly advancement characteristics of the East Asian summer monsoon with its interdecadal variations. Acta Geograph Sin 61(7):675–686

Jiang W, Song L, Wang S, Lv J (2009) Study on summer anomalies of precipitation and climatic causes in the Yangtze River Delta. Sci Meteorol Sin 29(3):355–361

Jiang J, Sun W, Pei X (2012) Climate change and possible reasons in Yangtze River Delta region in recent 50 years. Meteorol Disaster Reduction Res 35(4):17–25

Jones JR, Schwartz JS, Ellis KN, Hathaway JM, Jawdy CM (2015) Temporal variability of precipitation in the Upper Tennessee valley. J Hydrol 3:125–138

Kendall MG (1975) Rank correlation methods. Charles Griffin, London

Li W, Chen S, Chen G, Sha W, Luo C, Feng Y, Wen Z, Wang B (2011) Urbanization signatures in strong versus weak precipitation over the Pearl River Delta metropolitan regions of China. Environ Res Lett 6(3):1–9

Liang L, Li L, Liu Q (2011) Precipitation variability in Northeast China from 1961 to 2008. J Hydrol 404(1–2):67–76

Liu W, Tang B (2011) A hybrid time-frequency method based on improved Morlet wavelet and auto terms window. Expert Syst Appl 38(6):7575–7581

López-Moreno JI, Vicente-Serrano SM, Angulo-Martínez M, Beguería S, Kenawy A (2010) Trends in daily precipitation on the northeastern Iberian Peninsula, 1955–2006. Int J Climatol 30(7):1026–1041

Lv J, Ju J, Jiang J (2009) Interdecadal regime shifts of regional precipitation over eastern China during the last 100 years. J Atmos Sci 33(3):524–536

Mann H (1945) Non-parametric tests against trend. Econometrica 13: 245–259

Martinez CJ, Maleski JJ, Miller MF (2012) Trends in precipitation and temperature in Florida, USA. J Hydrol 452–453:259–281

Mei W, Yang X (2005) Trends of precipitation variations in the mid-lower Yangtze River Valley of China. J Nanjing Univ 41(6):577–589

Mishra AK, Singh VP (2010) Changes in extreme precipitation in Texas. J Geophys Res 115:D14106. doi:10.1029/2009JD013398

O'Gorman PA, Schneider T (2009) The physical basis for increases in precipitation extremes in simulations of 21st-century climate change. Proc Natl Acad Sci U S A 106:14773–14777

Pan A, Wang K, Zeng Y, Xie Z, Miao Q (2011) Trends of temperature and precipitation variation in the Yangtze River Delta from 1961 to 2006. Trans Atmos Sci 34(2):180–188

Pataki DE, Bowling DR, Ehleringer JR (2003) Seasonal cycle of carbon dioxide and its isotopic composition in an urban atmosphere: an thropogenic and biogenic effects. J Geophys Res 108(D23):3047–3049

Pathirana A, Denekew HB, Veerbeek W, Zevenbergen C, Banda AT (2014) Impact of urban growth-driven landuse change on microclimate and extreme precipitation—a sensitivity study. Atmos Res 138:59–72

Petrie MD, Collins SL, Gutzler DS, Moore DM (2014) Regional trends and local variability in monsoon precipitation in the northern Chihuahuan Desert, USA. J Arid Environ 103:63–70

Roy SS, Balling RC (2004) Trends in extreme daily precipitation indices in India. Int J Climatol 24(4):457–466

Roy SS, Rouault M (2013) Spatial patterns of seasonal scale trends in extreme hourly precipitation in South Africa. Appl Geogr 39:151–157

Sang Y, Wang Z, Li Z, Liu C, Liu X (2013) Investigation into the daily precipitation variability in the Yangtze River Delta, China. Hydrol Process 27:175–185

Sarr MA, Zoromé M, Seidou O, Bryant CR, Gachon P (2013) Recent trends in selected extreme precipitation indices in Senegal—a changepoint approach. J Hydrol 505:326–334

Shem W, Shepherd M (2009) On the impact of urbanization on summertime thunderstorms in Atlanta: two numerical model case studies. Atmos Res 92(2):172–189

Shepherd JM (2006) Evidence of urban-induced precipitation variability in arid climate regimes. J Arid Environ 67(4):607–628

Shi X, Xu X (2008) Interdecadal trend turning of global terrestrial temperature and precipitation during 1951–2002. Prog Nat Sci 18(11): 1383–1393

Shi N, Zhu Q, Wu B (1996) The East Asian summer monsoon in relation to summer large scale weather–climate anomaly in China for last 40 years. Sci Atmos Sin 20(5):575–583

Song X, Zhang J, AghaKouchak A, Roy SS, Xuan Y, Wang G, He R, Wang X, Liu C (2014) Rapid urbanization and changes in spatiotemporal characteristics of precipitation in Beijing metropolitan area. J Geophys Res Atmos 119(11):250–271

Svensson C (1999) Empirical orthogonal function analysis of daily rainfall in the upper reaches of the Huai River basin, China. Theor Appl Climatol 62:147–161

Tebaldi C, Hayhoe K, Arblaster JM, Meehl GA (2006) Going to the extremes. Clim Chang 79(3–4):185–211

Wang Q (2012) Homogeneity and comparison of approaches for spatial interpolation of temperature and precipitation data in Jiangxi Province China. Quatern Int 279–280:527

Wang W, Xing W, Yang T, Shao Q, Peng S, Yu Z, Yong B (2013) Characterizing the changing behaviours of precipitation concentration in the Yangtze River Basin, China. Hydrol Process 27(24): 3375–3393

Wei F (2008) Modern climatic statistical diagnosis and prediction technology, 2nd edn. China Meteorological Press, Beijing

Weldeab S, Lea DW, Oberhänsli H, Schneider RR (2014) Links between southwestern tropical Indian Ocean SST and precipitation over southeastern Africa over the last 17 kyr. Palaeogeogr Palaeoclimatol Palaeoecol 410:200–212

Wu G, Wang N, Hu S, Tian L, Zhang J (2008) Physical geography, 4th edn. Higher Education Press, Beijing, p 113

Xu J (2006) Quantitative geography. Higher Education Press, Beijing

Xu Y, Xu J, Ding J, Chen Y, Yin Y, Zhang X (2010) Impacts of urbanization on hydrology in the Yangtze River Delta, China. Water Sci Technol 62(6):1221–1229

Yang L, Villarini G, Smith JA, Tian F, Hu H (2013) Changes in seasonal maximum daily precipitation in China over the period 1961–2006. Int J Climatol 33:1646–1657

Zhai P, Zhang X, Wan H, Pan X (2005) Trends in total precipitation and frequency of daily precipitation extremes over China. J Clim 18(7): 1096–1108

Zhang J, Wei F, Liu S, Gao C (2008) Possible effect of ENSO on annual sediment discharge of debris flows in the Jiangjia Ravine based on Morlet wavelet transforms. Int J Sediment Res 23(3):267–274

Zhang Q, Xu C, Zhang Z, Chen Y, Liu C (2009) Spatial and temporal variability of precipitation over China, 1951–2005. Theor Appl Climatol 95(1–2):53–68

Zhang Q, Peng J, Xu C, Singh VP (2013) Spatiotemporal variations of precipitation regimes across Yangtze River basin, China. Theor Appl Climatol 115:703–712

Zhang Y, Smith JA, Luo L, Wang Z, Baeck ML (2014) Urbanization and rainfall variability in the Beijing metropolitan region. J Hydrometeorol 15(6):2219–2235

Zhao W, Zhang N, Tang J (2011) Analyses on precipitation characteristics in the Yangtze River Delta city belt based on the satellite data. Plateau Meteorol 30(3):668–674

Zhu Z, Yan R, Luo L (2009) Detection of signal transients based on wavelet and statistics for machine fault diagnosis. Mech Syst Signal Process 23(4):1076–1097

Zolina O, Simmer C, Gulev SK, Kollet S (2010) Changing structure of European precipitation: longer wet periods leading to more abundant rainfalls. Geophys Res Lett 37:L06704. doi:10.1029/2010GL042468